Published online 21 March 2013

Nucleic Acids Research, 2013, Vol. 41, No. 9 ***e103***
doi:10.1093/nar/gkt165

The effect of hybridization-induced secondary structure alterations on RNA detection using backscattering interferometry

Nicholas M. Adams[1,2], Ian R. Olmsted[1], Frederick R. Haselton[2], Darryl J. Bornhop[2,3,*] and David W. Wright[1,*]

[1]Department of Chemistry, Vanderbilt University, Nashville, TN 37235, USA, [2]Department of Biomedical Engineering, Vanderbilt University, Nashville, TN 37235, USA and [3]Vanderbilt Institute for Chemical Biology, Vanderbilt University, Nashville, TN 37232 USA

Received November 16, 2012; Accepted February 21, 2013

ABSTRACT

Backscattering interferometry (BSI) has been used to successfully monitor molecular interactions without labeling and with high sensitivity. These properties suggest that this approach might be useful for detecting biomarkers of infection. In this report, we identify interactions and characteristics of nucleic acid probes that maximize BSI signal upon binding the respiratory syncytial virus nucleocapsid gene RNA biomarker. The number of base pairs formed upon the addition of oligonucleotide probes to a solution containing the viral RNA target correlated with the BSI signal magnitude. Using RNA folding software *mfold*, we found that the predicted number of unpaired nucleotides in the targeted regions of the RNA sequence generally correlated with BSI sensitivity. We also demonstrated that locked nucleic acid (LNA) probes improved sensitivity approximately 4-fold compared to DNA probes of the same sequence. We attribute this enhancement in BSI performance to the increased A-form character of the LNA:RNA hybrid. A limit of detection of 624 pM, corresponding to $\sim 10^5$ target molecules, was achieved using nine distinct ~23-mer DNA probes complementary to regions distributed along the RNA target. Our results indicate that BSI has promise as an effective tool for sensitive RNA detection and provides a road map for further improving detection limits.

INTRODUCTION

The expression of single-stranded RNA is an essential part of the life cycle of human pathogens. RNA is found in great abundance during critical stages of infection. Some virus infections produce 10^3–10^4 detectable RNA molecules per virion (1,2). Additionally, a high degree of pathogen-specificity can be found in sequences of expressed RNA. Pathogen species and strains can be identified based solely on the detection of RNA sequences as short as 16 nt (3,4). Because of their abundance and species-specificity, RNA biomarkers are especially useful for pathogen detection and diagnosis of illnesses that result from pathogen infection. We have developed an interferometric method for RNA detection that is based on specific interactions with unlabeled oligonucleotide probes in solution.

Many methods have been developed to detect RNA biomarkers. Reverse transcription followed by polymerase chain reaction (RT-PCR) is a common technique used to quantify RNA. Because of its sensitivity, it has become the gold standard for RNA detection. PCR-based methods, however, typically require purification, denaturation, and time consuming amplification and labeling. Fluorescence-based methods, such as microarrays or molecular beacons, are also commonly used for detecting RNA targets using oligonucleotide probes (5), yet they often lack the sensitivity needed for diagnostic applications. Other nucleic acid probe-based methods developed for RNA detection include the biobarcode-assay (6), cantilever array sensors (7) and surface plasmon resonance (SPR) (8). These methods require complex probe synthesis procedures, nucleic acid labeling or immobilization, or specialized instrumentation and are deficient in terms of speed, sensitivity, convenience and/or cost. There is, therefore, a need for methods that are simple, rapid and sensitive for RNA detection. Backscattering interferometry (BSI) is a technology that circumvents the limitations of other detection methods as it has a simple instrumental design, does not require molecular labeling or amplification, and can be

*To whom correspondence should be addressed. Tel: +1 615 322 2636; Fax: +1 615 343 1234; Email: david.wright@vanderbilt.edu
Correspondence may also be addressed to Darryl J. Bornhop. Tel: +1 615 322 4404; Fax: +1 615 343 1234; Email: darryl.j.bornhop@vanderbilt.edu

The authors wish it to be known that, in their opinion, the first two authors should be regarded as joint First Authors.

performed in solution using microliter volumes in complex matrices.

BSI has been used to successfully monitor binding interactions of a variety of biological molecules with high sensitivity (9–15). The design of this unique interferometer is very simple. A He–Ne laser is used to illuminate a semi-circular microfluidic channel containing <1 µl of analyte, creating a set of high contrast interference fringes of reflected and refracted light (Figure 1A). When a specific binding event occurs, the refractive index (RI) of the solution in the channel changes, causing these fringes to shift in a manner that is proportional to the concentration of the analyte (Figure 1B–C). Though BSI has been used to quantify protein biomarkers via antibody–antigen interactions (10), the work presented here represents the first report of its use for detecting and quantifying RNA biomarkers.

Nucleic acid probes of various lengths and chemical compositions can be designed to complement any sequence of a target nucleic acid; therefore, the design space of nucleic acid probes is extremely large compared to other types of probes, such as antibody-antigen or even aptamer–ligand interactions, which require specific and constrained tertiary structures for target recognition. Additionally, commercial synthesis of oligonucleotides is widely available and is able to produce virtually any sequence of natural or chemically modified nucleotides. Compared to other biomolecular probes (e.g. antibodies), nucleic acids also have relatively modest chemical complexity and are uniformly charged. These properties reduce variations in RI that may result from the interactions of the probes with the solvent, making them ideal probes for biomarker detection using BSI. Furthermore, nucleic acids are not 'sticky' like proteins, reducing artificial signals from non-specific interactions, such as binding to the channel wall.

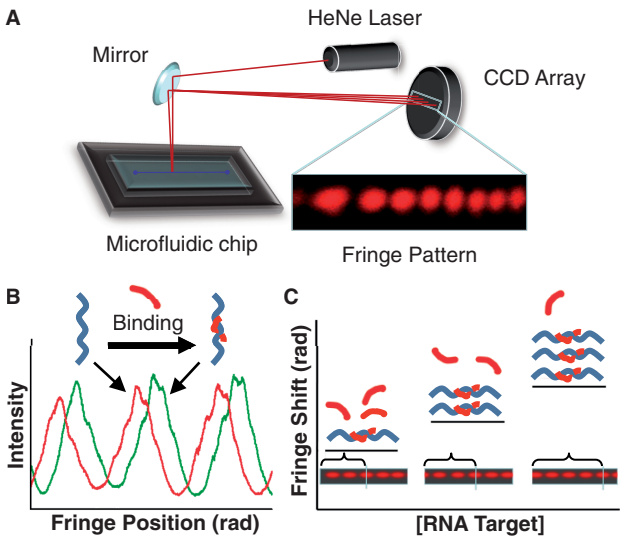

Figure 1. Depiction of the optical train and mechanism of signal generation for RNA detection using BSI. (**A**) Schematic of BSI optical train. (**B**) Digital representation of interference fringes. (**C**) Representation of signal generation as DNA probes bind complementary RNA targets.

An important property of BSI in the context of biomarker detection is its large dynamic range. The optical properties of the interferometer are such that the fringes continue to shift (i.e. produce a signal) as long as a change in RI occurs and that the RI of the fluid differs from that of the microfluidic chip. Consequently, the dynamic range of BSI can be expanded as long as there are analytes available to bind and change the RI. BSI sensitivity can therefore be dramatically enhanced without reaching signal saturation. This property is in contrast to detection assays that are dependent on light intensity, in which photometers can become saturated with extreme amplification methodologies. Oligonucleotide probes that are designed to produce the maximum change in RI upon binding the RNA target will, therefore, provide maximum BSI signal and optimize sensitivity. In this report, we have investigated the utility of BSI for label-free detection of a specific viral RNA biomarker sequence in solution. We focus on the respiratory syncytial virus (RSV) nucleocapsid (N) gene RNA, a biomarker with which our laboratories have had considerable experience (1,16,17). A systematic evaluation of a subset of oligonucleotide probe design parameters was conducted to determine interactions and characteristics of nucleic acid probes that enhance the sensitivity of BSI for detecting this RNA biomarker.

MATERIALS AND METHODS

Preparation of the synthetic RNA targets

The RNA target used in these studies is a synthetic ~1300 nt positive-sense RNA molecule of the RSV strain A_2 N gene. The RNA was prepared as previously described (1). Briefly, a pGBKT7 vector containing the RSV N gene insert was amplified in *Escherichia coli* strain DH5α, purified using a Qiagen Plasmid Midi Kit, linearized with the BssHII restriction enzyme, reverse transcribed using the Ambion T7MEGAscript transcription kit, and treated with DNase I. The integrity and length of the RNA product was confirmed using denaturing agarose gel electrophoresis. Aliquots of the RNA were stored at a concentration of ~80 nM in Tris-EDTA buffer at −80°C until they were used. The RNA mismatch targets used in these studies were commercially synthesized at a 50 nmole scale and desalted by Sigma-Aldrich. The sequences of the full-length RNA target and the mismatch targets used in these studies are provided in Supplementary Figure S1.

Synthesis of the oligonucleotide probes

The DNA oligonucleotide probes used in these studies were commercially synthesized at a 200 nmole scale by Sigma-Aldrich and purified using reverse phase cartridge purification. Locked nucleic acid (LNA) oligonucleotide probes were synthesized at a 250 nmole scale by Exiqon and purified with high performance liquid chromatography. Each lyophilized oligonucleotide was resuspended to a concentration of ~100 µM in molecular grade water (Fisher) and stored at −20°C until they were used. The

sequence of each oligonucleotide probe used in these studies is provided in Supplementary Table S1.

Backscattering interferometry

Details of the BSI instrumental configuration have been described in detail previously (9). In brief, a 5 mW helium neon laser ($\lambda = 635$ nm) is directed onto a borosilicate glass microfluidic chip etched with a near-semicircular channel that is about 210 μm wide and 100 μm deep. The coherent, collimated light source reflects and refracts within the channel, creating a fringe pattern that is detected with a linear CCD array. The fringes shift spatially with respect to the RI of the solution, and the position of a select group of fringes is analysed with an in-house LabView-based fast Fourier transform analysis program (18).

Unless otherwise noted, all assays were performed in an end-point format where a fixed concentration of probe (100 nM) was incubated with increasing concentrations (0–36.5 nM) of target RNA in Tris-buffered saline. Samples were mixed with a pipette and incubated at room temperature for 2.5 h to ensure that the binding equilibrium was reached. One microliter of each sample was sequentially injected into the microfluidic channel and the signal was recorded for 30 s. To correct for bulk RI changes, a series of blank measurements were taken from samples containing increasing concentrations of RNA target in the absence of probe. These values were then subtracted from the sample signal. The RI shift, measured in radians, was then plotted against the concentration of the target to produce a binding response curve. The slope of the binding response curve, in radians (rad) per nanomolar, was used as a measure of sensitivity. The lower limit of detection (LOD) was calculated using the following equation:

$$\mathrm{LOD} = 3 \times \sigma \,/\, \mathrm{slope},$$

where σ is the average of three standard deviation measurements at each RNA target concentration tested and the slope is the best-fit trendline of the linear range of the binding curve ($y = ax + b$).

Quantification of net nucleic acid hybridization

The relative amount of nucleic acid hybridization was quantified using a SYBR Green assay. Samples were prepared in triplicate with 1 nM of the synthetic RSV N gene RNA, 10 nM of the probe or probes, and a 1:9000 dilution of SYBR Green I (Life Technologies). Samples for the blank measurements were prepared in triplicate without RNA or without the DNA probes. For the LNA:RNA and DNA:RNA hybridization comparison, samples were prepared in triplicate using 60 nM LNA or DNA, 20 nM RNA complement of the same length, and a 1:9000 dilution of SYBR Green I (Life Technologies). A standard curve of double-stranded DNA of the same sequence and length was used to approximate the percent hybridization in the LNA:RNA and DNA:RNA samples. Prior to the addition of SYBR Green I, each sample was heated to 90°C for 5 min and cooled slowly to room temperature over the course of 1 h. Fluorescence measurements were recorded using a BioTek Synergy H4 Hybrid 96-well plate reader using an excitation wavelength of 497 nm and a detection wavelength of 520 nm. The values were normalized by subtracting signal of the samples from the background signal generated in the RNA-alone or the DNA-alone blank samples.

Preparation of and evaluation of surrogate nasal wash samples

HEp-2 cell lysates were prepared in a manner previously described (1). Briefly, cells were cultured to a confluent monolayer in a cell culture flask, harvested and resuspended in a cell lysis/RNA preservation solution (4 M guanidinium thiocyanate, 25 mM sodium citrate [pH 7.0] 0.5% N-laurosylsarcosine [Sarkosyl], 0.1 M 2-mercaptoethanol), and stored at −80°C. The surrogate nasal wash samples were prepared by diluting the cell lysates into phosphate buffered saline at 1×10^5, 5×10^4, 1×10^4 and 0 cells/ml concentrations and spiking each with the synthetic ~1300 nt RSV N gene RNA biomarker at a final concentration of ~16 nM.

For evaluation of the RNA target in the surrogate nasal wash samples using BSI, the samples were split into two halves. One half of each sample was used for total RNA extraction, and the other half was left unextracted. Total RNA extraction was performed using a self-contained continuous tubing extraction cassette as previously described (1). Briefly, each sample was added to an RNA binding solution containing silica-coated magnetic beads. The beads were mixed with the sample for 5 min and then drawn through a series of RNA extraction solutions. Total RNA was eluted into water, and quantification of the synthetic ~1300 nt RSV N gene RNA biomarker was performed using BSI. To validate the BSI results, quantitative reverse-transcription polymerase chain reaction (qRT-PCR) was performed on the same sample set. Each sample was extracted and evaluated in triplicate for BSI and qRT-PCR determinations. qRT-PCR was performed as described previously (1).

RNA folding analysis

The folding state of the synthetic RSV N gene RNA was predicted using the RNA Folding Form of the *mfold* software package available online (http://mfold.rna.albany.edu/?q=mfold/RNA-Folding-Form). The full-length sequence of the target (1331 nt, sequence available in Supplementary Figure S1) was used as the input, and the default settings were used. The five structures predicted to have the lowest energy were used to identify the folding state at the probe binding sequences. The number of consecutive unpaired bases for each of these sequences were averaged from the five predicted structures and plotted against the slope of the linear range of the BSI response curve. The five lowest energy *mfold* RNA folding structures are provided in Supplementary Figure S2.

Nucleic acid secondary structure determination

Circular dichroism (CD) spectra were collected using an Aviv CD spectrometer model 215 (Aviv Biomedical, Inc.). To compare the LNA:RNA, DNA:RNA and DNA:DNA hybrids, solutions were prepared in 40 μl volumes

containing 30 μM of DNA, RNA and/or LNA strands in Tris-buffered saline. Prior to collecting CD spectra, each sample was heated to 90°C for 5 min and cooled slowly to room temperature over the course of 1 h. For the A-form to B-form transition study, a solution of 80% 2,2,2-Trifluoroethanol (TFE) containing 385 μM Tris-HCl, 38.5 EDTA, 5 mM NaCl and 12 μM of each DNA strand was prepared. Prior to adding the TFE, the solution was heated to 90°C for 5 min and cooled slowly to room temperature over the course of 1 h. TFE was added stepwise accompanied by immediate mixing to avoid DNA precipitation while transitioning to A-form DNA. The concentration of TFE was diluted to 77.5, 75, 72.5 and 70% to by adding the appropriate volumes of a solution containing 385 μM Tris-HCl, 38.5 EDTA, 5 mM NaCl and 12 μM of each DNA strand. At each TFE concentration, 60 μl of the sample was removed and CD and BSI measurements were immediately performed. Blank measurements were collected from solutions prepared at each TFE concentration and containing 385 μM Tris–HCl, 38.5 EDTA and 5 mM NaCl, with no DNA. All CD spectra were collected from 320 nm to 200 nm wavelengths at 25.0°C in a 1.0 mm pathlength quartz cuvette using a 0.5 nm wavelength step, a 1.0 nm bandwidth, and a 1 s averaging time. Spectra were averaged from at least three separate scans, smoothed and normalized using CD-215 software version 2.90 provided by the manufacturer.

RESULTS

Enhanced BSI sensitivity using 22-mer probes

The design space of oligonucleotide probes targeting the ~1300 nt RSV N gene RNA biomarker sequence is extremely large. Oligonucleotides of virtually any length and sequence complementary to the target could be used, and a variety of chemically modified nucleotides could be substituted for natural nucleotides. Because an exhaustive study of all the potential probe designs is not feasible, we conducted a systematic evaluation of a subset of oligonucleotide probe design parameters. The first probe investigated was RSVN(242–263), a 22-mer DNA probe with a sequence chosen based on previous success as a primer for PCR studies aimed at amplifying RSV N gene cDNA. BSI measurements using the RSVN(242–263) 22-mer probe produced a linear response proportional to the concentration of the RSV N gene RNA with a LOD of 3.73 nM target RNA (Figure 2A and Table 1). As a negative control, a scrambled sequence of the same 22-mer was evaluated under the same conditions and yielded negligible signal. Postulating that probe length would impact BSI signal, probes RSVN(242–256), RSVN(242–285) and RSVN(242-329) were tested, which are 15, 44 and 88 nt in length, respectively, and start from the same position in the target RNA as the 22-mer probe. Each of these probe lengths resulted in slightly less signal and poorer detection limits than the 22-mer probe. To relate the BSI signal to a net increase in base pairs, the relative hybridization of these probes to the RNA target was determined using a SYBR Green assay (Figure 2B).

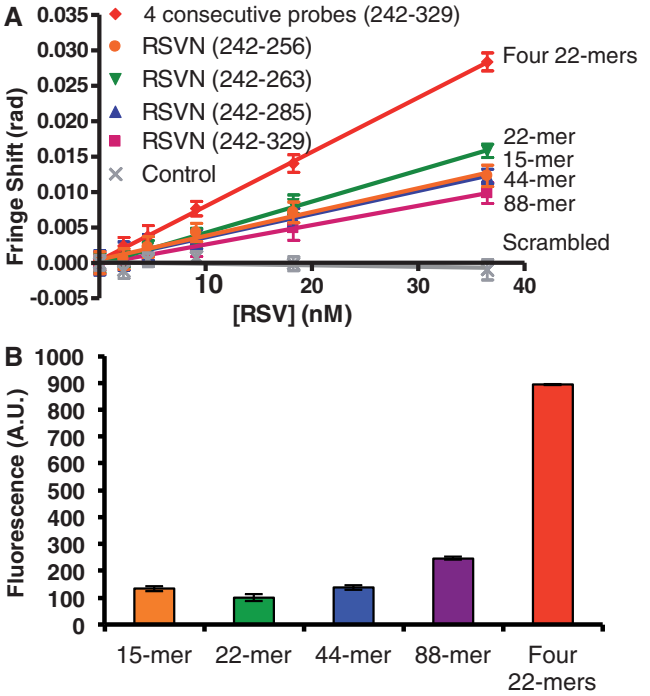

Figure 2. Comparison of the BSI binding response and net hybridization upon adding the 15-mer, 22-mer, 44-mer, 88-mer or four consecutive 22-mer DNA probes to the RNA target. (**A**) The probe length that produces optimal BSI signal is 22 nt. Four short 22-mer DNA probes have improved signal over one 88-mer spanning the same target sequence. A scrambled negative control sequence produced negligible signal. (**B**) Net hybridization of the four consecutive 22-mers is significantly greater than any of the four probe lengths.

Table 1. Summary of the slopes of the binding curves and limits of detection for each probe combination tested

Probe	Slope ($\times 10^{-5}$)	LOD (nM)
RSVN(242–263)	44	3.73
RSVN(242–256)	30	26.7
RSVN(242–285)	33	5.16
RSVN(242-–329)	27	8.96
Four consecutive DNA probes	77	2.04
Four distributed DNA probes	250	2.54
Nine distributed DNA probes	627	0.624
RSVN(264–285)	246	5.78
RSVN(286–307)	25	68.4
RSVN(308–329)	359	4.52
RSVN(1070–1091)	84	15.0
RSVN(800–821)	52	35.6
RSVN(755–774)	27	146
RSVN(242–263)L	175	2.15
Four distributed LNA probes	349	1.05

The signal generated from the intercalation of SYBR Green dye in the 15-mer, 44-mer and 88-mer probe:target hybrids was slightly greater than that of the 22-mer probe:target hybrid. Interestingly, we discovered that by dividing the 88-mer probe into four contiguous 22-mer probes, the slope of the BSI response was significantly increased, resulting in a LOD of 2.04 nM target RNA, or $\sim 4.1 \times 10^5$ molecules. This enhancement in sensitivity was reflected by the increase in the net hybridization of the

four consecutive 22-mers compared to the 15-mer, 22-mer, 44-mer and 88-mer probes (Figure 2 and Table 1). These results indicate that of the probes tested, the optimal length is 22 nt for BSI detection and that the BSI signal can be enhanced using multiple probes of that length.

Enhanced BSI sensitivity using multiple distributed probes

Next we investigated the influence on assay sensitivity of distributing the probes along the ~1300 nt RNA target sequence. Because the four consecutive probes were designed to bind contiguous sequences of the target RNA, it was hypothesized that the conformation of the target RNA secondary structure prevented the probes from fully hybridizing and that distributed sequences would improve signal. By distributing the four probes along the length of the target RNA, the slope of response was improved more than 3-fold over the four contiguous sequences (Figure 3A and Table 1). Furthermore, increasing the total number of probes to nine further improved sensitivity, providing a LOD of 624 pM, or 1.5×10^5 molecules target RNA. Accordingly, studies evaluating the net hybridization of the single probe versus the four and nine probe combinations revealed increased hybridization with the increased number of probes (Figure 3C), further validating that BSI signal is at least partially the result of a net change in hybridization.

To further demonstrate that the increased signal from the nine-probe cocktail was a result of an increase in the number of available binding sites, as opposed to the effect of having a higher concentration of probes present, a saturation binding isotherm was constructed for both the single probe and the nine-probe cocktail. For this assay, the concentration of the *target RNA* was held constant while the probe concentration was varied from 0–100 nM. The signal at saturation (B_{max}) for the single probe was 0.087 radians, whereas the signal for the nine distributed probes was 0.25 radians, a 2.9-fold overall increase in signal (Figure 4). This result indicates that the sensitivity improvement observed in the nine-probe system is the result of an increased number of available binding sites; therefore, a greater number of binding events can occur before target saturation is reached. This may not be surprising as BSI signal magnitude is directly related to the number of binding events (9). These data are consistent with these previous observations and indicate that the greatest BSI sensitivity over a large dynamic range is achieved by maximizing the number of available target RNA binding sites.

Target specificity is maintained in RNA samples extracted from complex matrices

To evaluate the specificity of BSI using the 22-mer RSVN(242–263) DNA probe, six 22-mer RNA targets containing 0, 1, 3, 5, 7 and 10 mismatched nucleotides distributed throughout the sequence were tested in an end-point assay format (Figure 5A). With an increasing number of mismatched nucleotides in the target sequence, BSI signal dropped off significantly, resulting in essentially no signal using the RNA target containing 10 mismatched bases in the sequence. The signal produced using the RNA target sequences containing 1 and 3 mismatches was statistically equal to that of the 0 mismatch target ($P = 0.5$ and 0.14, respectively). The signal from the targets containing 5, 7 and 10 mismatches was statistically different from the 0 mismatch control ($P < 0.05$).

To examine the specificity of BSI in samples containing a high background non-target molecules, we tested BSI for detecting the synthetic ~1300 nt RNA target spiked into surrogate nasal wash samples containing increasing background concentrations of HEP-2 cell lysate (Figure 5B). In extracted samples (i.e. samples of total

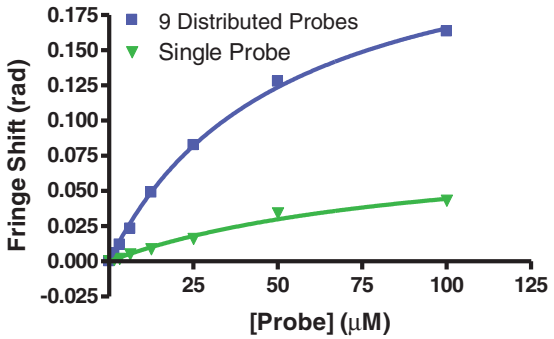

Figure 4. Saturation curves of target RNA incubated with increasing concentrations of either a single 22-mer probe or a mixture of nine distributed probes. The mixture of nine probes saturates at a higher level than the single probe.

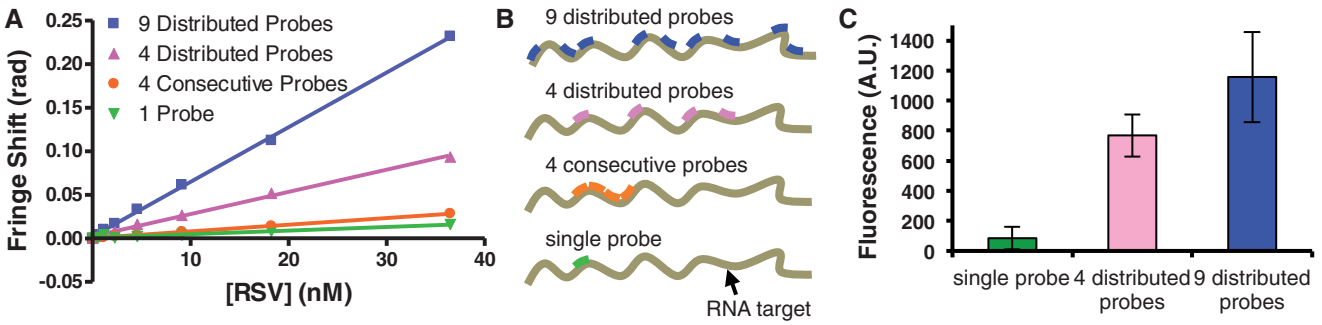

Figure 3. Comparison of the BSI binding response and net hybridization of various numbers and distributions of probes incubated with the RNA target. (**A**) Increasing the number and distribution of distinct probes improves sensitivity. (**B**) Illustration of the relative positions of the DNA probes along the RNA target. (**C**) Hybridization studies confirm that increased number of probes bound correlates with increased binding signal.

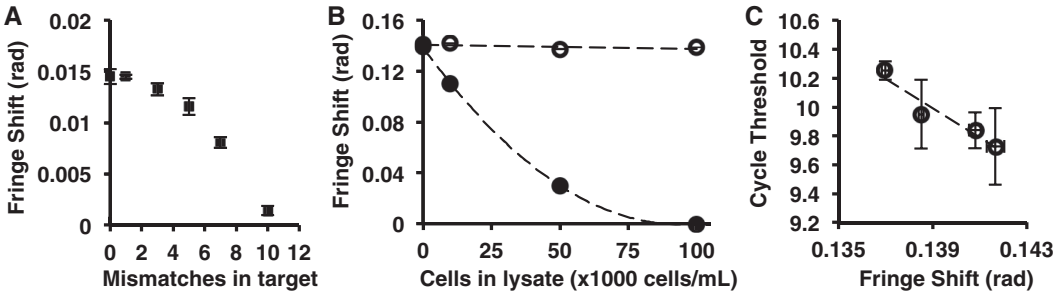

Figure 5. Evaluations of BSI specificity for (**A**) mismatched targets or (**B**) RNA targets in complex samples using a single 22-mer probe. (A) BSI signal drops off moderately when probing for RNA targets with increasing numbers of mismatched nucleotides. (B) BSI signal is consistent when probing for the ~1300 nt RNA biomarker in a sample of total RNA extracted from HEp-2 cell lysates of increasing concentrations (open circles), whereas BSI signal diminishes in unextracted samples of increasing background concentration (closed circles). (C) qRT-PCR cycle threshold values for the extracted samples correlate with the BSI fringe shift values ($R^2 = 0.92$).

RNA isolated from the cell lysate background), the signal produced was consistent despite the increase in the total background RNA extracted from the samples. Notably, cycle threshold values of qRT-PCR analysis of the extracted RNA samples correlated strongly with the fringe shift values of BSI (Figure 5C), suggesting that the quantitative potential of BSI for extracted RNA biomarkers at this concentration is equivalent to qRT-PCR. In unextracted samples (i.e. samples of RNA spiked into cell lysate background), BSI signal diminished with increasing cell lysate concentration, resulting in no distinguishable signal in the highest concentration of cell lysate evaluated (Figure 5B). Taken together, these data suggest that BSI detection of RNA is tolerant of some mismatched nucleotides in the target sequence, yet specificity is retained in total RNA extracts from complex cell lysate samples.

RNA target folding affects BSI binding signal

During the process of testing a variety of oligonucleotide probe sequences, we observed that probes of similar length (i.e. 20–22 nt) and nucleotide content, but composed of different nucleotide sequences, yielded significantly disparate BSI binding responses. Because BSI sensitivity is produced in part by changes in conformation (8), we surmised that the probes were not only interacting at the primary sequence level of the target RNA (i.e. base pairing), but that probe binding signal was also impacted by the complex folding state of the RNA target. To investigate the effects of RNA target folding on BSI response, *mfold* software was used to predict secondary structure motifs in the regions complementary to the probes that would account for the variation in probe binding. Specifically, the software was used to identify regions of the RNA target that are predicated to be open loops, or sequences that would be available to bind a complementary oligonucleotide probe. Although *mfold* cannot predict RNA folding with absolute certainty, with the exception of two probes tested, we found a positive correlation between the number of unpaired nucleotides in the open loop regions of the predicted structure of the RNA target and the BSI signal produced by the probe complementary to that sequence (Figure 6). In line with probe design software for microarray oligonucleotide

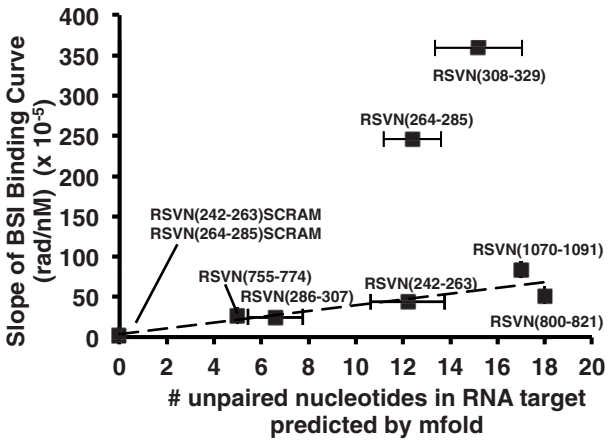

Figure 6. DNA probes designed to bind different regions of the RNA target generate a range of BSI binding responses. With the exception of two probes, binding response correlates positively with the number of nucleotides predicted to be unpaired in the RNA target ($R^2 = 0.86$). *x*-axis values are averages of predicted unpaired nucleotides in the five lowest energy folding structures of *mfold* ± standard error.

sequences (4), probes designed to bind RNA target sequences predicted to be single-stranded would result in the greatest net change in hybridization and produce the greatest change in BSI signal. Probes RSVN(264–285) and RSVN(308–329), however, produced a much higher signal that does not appear to fit this model. One possible explanation for the large signal of these probes, compared to the other probes, is that tertiary structure rearrangements or allosteric changes in the RNA target may be occurring upon probe binding. We have observed similar binding-order related signal enhancements in other systems, particularly with thrombin binding aptamers (12). These observations cannot be fully explained due to limitations in the current model, but are under investigation.

Enhanced BSI sensitivity using LNA probes

With some knowledge of the probe length and spacing parameters that yield good signal in BSI for optimized hybridization, we explored LNAs, a category of oligonucleotides with unique structure and binding characteristics. LNA oligonucleotides have much greater binding

affinities for their targets when compared to DNA or RNA of similar length and sequence (19). The first LNA probe we used, RSV(242–263)L, was the same sequence and length as the 22-mer DNA probe used in our initial experiments, except that every third nucleotide in the sequence contains a methylene group bridging the 2′ oxygen and the 4′ carbon of the ribose ring, 'locking' the sugar into the 3′-*endo* conformation. With these simple structural modifications, a 4-fold improvement in sensitivity was achieved over the DNA probes, resulting in a LOD of 2.15 nM of target RNA (Figure 7A and Table 1). Using a mixture of four *distributed* LNA probes, identical in sequence and length to the four distributed DNA probes, a LOD of 1.05 nM target RNA was achieved. These results compare favorably to the 1.5-fold improvement in LOD observed when increasing the number of DNA probes from one to four (Table 1). Interestingly, this improvement in signal and sensitivity was not attributed to an increase in the net hybridization of the probe to the RNA target. Although the increased affinity of LNA for the RNA target would generally shift the binding equilibrium toward the bound state, both LNA and DNA probes hybridize to approximately the same number of RNA targets (Figure 7B). This result is likely because the LNA and DNA probes are added to the RNA target in such excess that, despite the increased affinity of LNA for the target RNA, the total number of LNA and DNA probes bound to the RNA target was nearly equivalent. Because there is not a significant increase in net hybridization when using LNA probes, we concluded that hybridization alone did not account for the 4-fold improvement in BSI signal using the LNA probe. Therefore, we explored the possibility that the improvement in sensitivity was the result of the unique structural characteristics of LNA:RNA hybrid.

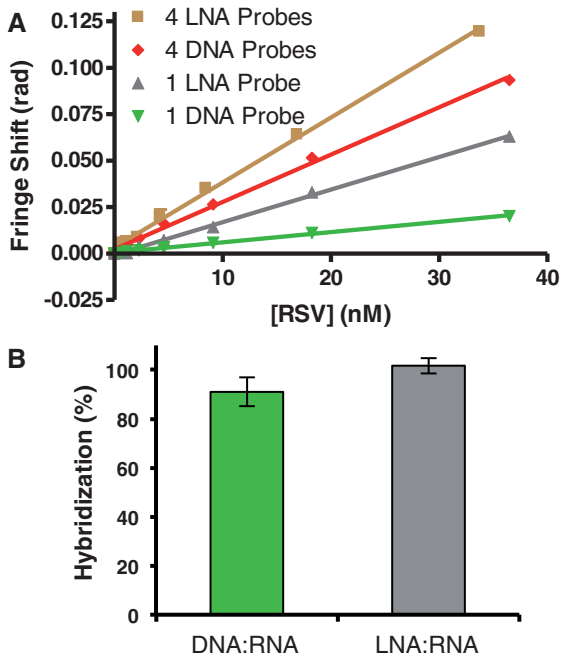

Figure 7. Comparison of the BSI binding response and net hybridization of LNA and DNA probes of the same sequence and length incubated with target RNA. (**A**) LNA probes improve the BSI signal. (**B**) DNA:RNA hybrids and LNA:RNA hybrids produce virtually the same net hybridization.

Induced A-form secondary structure improves BSI sensitivity

It has been established that LNA:RNA hybrids primarily form A-form secondary helical structures, whereas DNA:RNA hybrids consist of a mixture of A-form and B-form character (20). Since the net hybridization measured for DNA versus LNA probes binding the RNA target was approximately equivalent but the BSI signal of the LNA probes was significantly greater than that of the DNA probes (Figure 7A and B, respectively), we hypothesized that the induced A-form helical character of the LNA:RNA hybrid was responsible for the greater RI change upon formation compared to the DNA:RNA hybridization. Accordingly, we evaluated nucleic acid hybrids of the same length and sequence that exhibit a range of secondary structures using CD and BSI. To reduce the background noise from the unbound regions of the ~1300 RNA target, the RNA and DNA complements used in these studies are the same length as the LNA and DNA probes (22 nt). Based on the CD spectra, we verified that the LNA:RNA hybrid resulted in a characteristic A-form secondary structure, the

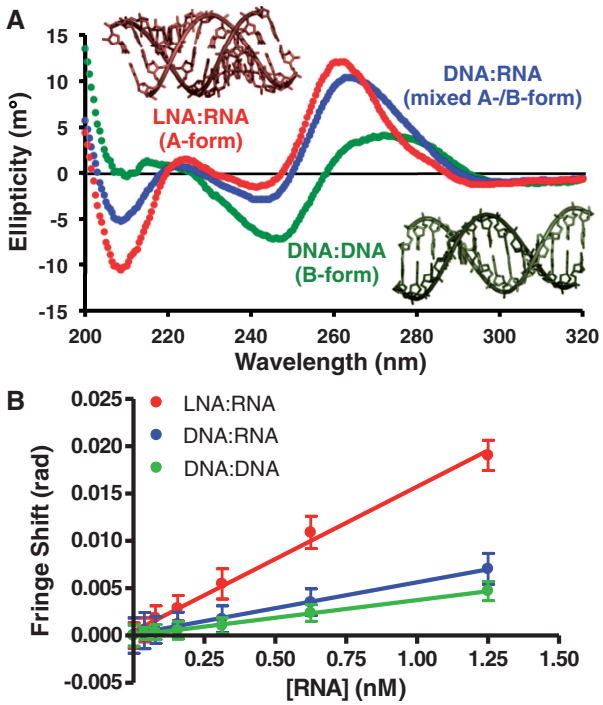

Figure 8. Relative degree of A-form nucleic acid character of the DNA:DNA, DNA:RNA and LNA:RNA hybrids corresponds with increased BSI signal. (**A**) The CD spectrum of the DNA:DNA duplex (green) corresponds to B-form secondary helical structure with a maximum near 280 nm, a deep minimum near 250 nm. LNA:RNA hybrid (red) produces a spectra corresponding to A-form secondary structure with a maximum near 270 nm and a shallow minimum near 245 nm. The DNA:RNA hybrid produces a spectra that is intermediate of A-form and B-form. (**B**) BSI binding curves of LNA:RNA, DNA:RNA and DNA:DNA.

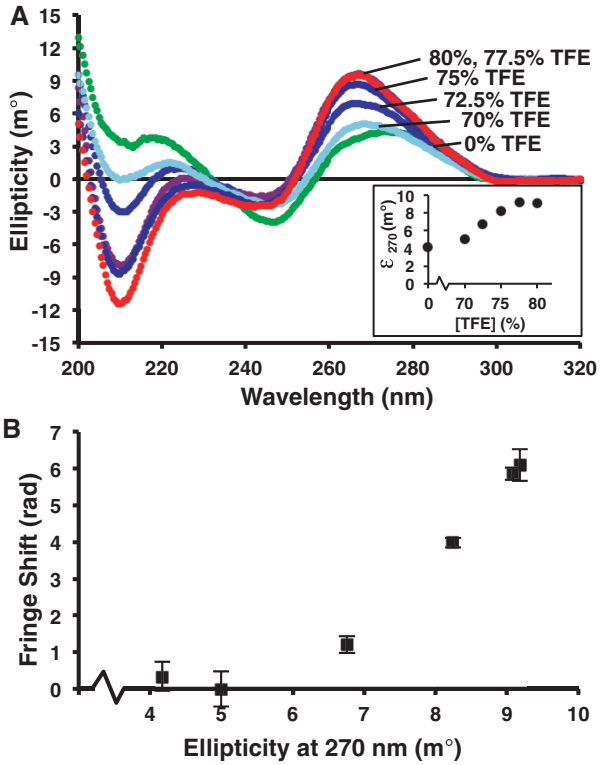

Figure 9. Relative degree of A-form character corresponds to increased BSI signal. (**A**) CD spectra of the DNA duplex demonstrate a shift from A-form to B-form structure with decreasing concentrations of TFE. *Inset*: A-form to B-form transition monitored at 270 nm. (**B**) Ellipticity at 270 nm correlates positively with the shift in the RI as detected by BSI.

DNA:RNA hybrid resulted in a secondary structure consisting of a mixture of A- and B-form, and the DNA:DNA duplex resulted in a characteristic B-form secondary structure (Figure 8A). These same hybrids were then evaluated using BSI. The LNA:RNA interaction produced the largest RI shift (1.53×10^{-2} rad/nM), followed by the DNA:RNA interaction (5.48×10^{-3} rad/nM), and the DNA:DNA interaction produced the smallest RI shift (3.75×10^{-3} rad/nM) (Figure 8B). These data indicate that the BSI signal or slope reflects the extent to which the hybridized product displays A-form secondary structure. These observations are consistent with the hypothesis that BSI signal can be maximized using oligonucleotide probes that induce the greatest net change in the nucleic acid secondary structure.

To further validate that the formation of A-form secondary structure is responsible for the observed increase in BSI signal, as opposed to the differences in the primary structures of the nucleotide subunits, we performed BSI measurements on a DNA:DNA duplex matching the sequence of the RSVN(242–263) probe at various stages of a TFE-induced B-form to A-form transition. Incubation with high concentrations of TFE is a well-established method for converting B-form secondary structure in DNA:DNA duplexes to A-form (21,22). TFE was titrated into a solution containing a DNA:DNA duplex and the secondary structure transition was confirmed by CD analysis (Figure 9A). BSI signal magnitude increased as the DNA:DNA duplex adopted a more A-form character as monitored by the ellipticity at 270 nm. These data validate the BSI signal enhancing effect of induced alterations to the helical geometry of the nucleic acid hybrid (Figure 9B).

DISCUSSION

In this study, we have demonstrated the application of BSI for the detection of a RSV N gene RNA biomarker in solution using unlabeled nucleic acid probes. These studies have shown that induced secondary structure formation is a major contributing factor to signal generation for detecting RNA with oligonucleotide probes by BSI. Several factors are important in obtaining a maximum signal to noise ratio. The number of binding events are an important factor, yet as we have previously shown with protein binding systems (9), the nature of the binding event (i.e. the resulting structure) also plays a critical role in BSI signal magnitude. The first and most obvious source of secondary structure formation is the net helical duplex formation that occurs when a nucleic acid probe hybridizes to the RNA target.

We found that the sensitivity of the assay is greatest when multiple, short probes are employed, distributed along the length of the RNA target (Figure 3 and Table 1), which results in the maximum number of binding events (Figure 3C). In comparison to a single 22-mer DNA probe which detects RNA target concentration at a sensitivity of 4.4×10^{-4} radians/nM (LOD = 3.73 nM); four DNA probes produce a 5.7-fold increase in sensitivity, or 2.50×10^{-3} radians/nM (LOD = 2.54 nM); and nine DNA probes produce a 14.3-fold increase in sensitivity, or 6.27×10^{-3} radians/nM (LOD = 624 pM) (Table 1). As one would expect, the increase in signal is directly proportional to the number of probes available to bind the RNA target.

Experiments aimed at studying the effects of probe length demonstrated that BSI signal magnitude was greatest using a probe length of 22 nt (Figure 2). Interestingly, though they contain the same number of base pairs, four contiguous 22-mer probes yield an appreciably larger signal than a single 88-mer probe. We postulate that steric hindrance resulting from the native structure of the ~1300 nt RNA target prevents the longer probe from binding as effectively as the four shorter probes. Additionally, in a multi-probe assay, it may be the case that some probes bind at a higher kinetic rate than others, altering the conformation of the target RNA and thus creating more favorable binding conditions for subsequent probes. We also found that while four short, adjacent probes create more binding signal than a single long probe, sensitivity is improved even further by distributing the probes along the length of the target. This may be explained by the potential for probes that target sequences immediately adjacent to prevent the other probes from binding because of the induced secondary structure and rigidity of the probe-bound sequences.

BSI was also effective in detecting the synthetic ~1300 RNA target from total RNA extracted from surrogate nasal wash samples of increasing background complexity

(Figure 5B and C), demonstrating the specificity of BSI for detecting target RNA, as the target only made up a portion of the total RNA extracted from the sample. In contrast, when using unextracted samples, BSI signal diminished with increasing background cell lysate concentration. We hypothesize that the complex bimolecular content present in unextracted cell lysate samples has a signal-suppressing effect on BSI as a result of aggregate non-specific interactions. These results demonstrate the potential for BSI to be used as a diagnostic tool for quantifying specific RNA biomarker sequences that have been extracted from complex samples. Despite the successful detection of a specific RNA target from a background of total RNA extract, BSI displayed moderate specificity using a series of mismatched RNA targets (Figure 5A). As the focus of this initial work has been centered on improving the sensitivity of BSI, there are many factors for optimization of specificity to be examined in future work.

It was determined that individual probes of similar nucleotide content and length did not produce a similar level of BSI signal. We found that the discrepancy in BSI signal produced from the various probe sequences can be partially explained with RNA folding predictions of the RNA target. For most RNA sequences, secondary structures are significantly more stable than tertiary structures and are more likely to contribute to the native structure of the RNA target (23). Therefore, only the secondary structure of the RNA target was evaluated in these studies. Using *mfold* software to predict the folding state of the RNA target, we found that probes targeting sequences predicted to have mostly unpaired nucleotides (i.e. open loops) generally produced more signal than probes targeting sequences predicted to be mostly double stranded. Two probes, however, produced exceptionally high signal compared to probes targeting regions of similar predicted secondary structure. Alterations in the tertiary structure of the RNA target induced by probe binding may explain the comparatively large signal changes produced by these probes. Future studies will be aimed at investigating the role of tertiary structure in BSI signal generation.

It was also found that the integration of 'locked' nucleotides into the DNA probe nearly quadruples the sensitivity of BSI (Figure 7 and Table 1). LNA has been widely used for nucleic acid probing applications (24–26). It has been reported that LNA has exceptional binding affinity for complementary RNA or DNA targets while maintaining or even improving sequence specificity (19). Because BSI detects changes in the RI that are induced by the binding of two molecules, the signal enhancement produced by LNA oligonucleotides could potentially have thermodynamic, structural and/or solvation explanations. Perhaps the most important characteristic of LNA oligonucleotides is the high thermal stability when duplexed with RNA. Melt temperatures of LNA:RNA hybrids can increase by $\sim$5°C per locked nucleotide incorporated into the sequence (24). Because of this high affinity for RNA, a higher proportion of LNA oligonucleotides should bind complementary targets compared to DNA of identical sequence and length. However, the amount of DNA and LNA probe used in these studies is in great excess relative to the number of available targets, which is intended to drive binding toward probe saturation. The hybridization studies confirmed that the relative amount of bound LNA probes is nearly the same as DNA probes at equilibrium (Figure 7B), indicating that the thermodynamic explanation is probably not the greatest contributor to the BSI signal enhancement.

The RI of a solution can also change when solutes undergo changes in structural conformation. When binding RNA, a single LNA nucleotide can perturb the surrounding DNA nucleotides to adopt the C3′-*endo* conformation. Consequently, LNA:RNA hybrids form homogeneous A-form helical secondary structures, whereas DNA:RNA hybrids generally form a heterogeneous mix of both A-form and B-form (20). Our secondary structural analysis of the nucleic acid hybrids using CD confirmed that the LNA:RNA hybrids formed A-form helical structure, whereas the DNA:RNA hybrid forms a mixture of A-form and B-form helical structures (Figure 8A). As another point of reference, we studied a DNA:DNA duplex with distinct B-form character as confirmed by CD. The increased sensitivity of BSI for detecting A-form hybrids, compared to the A-form and B-form mixed hybrid or the B-form duplex, indicates a structural basis for RI perturbation (Figure 8B). This was further validated through the measurements conducted on the TFE-induced A-form character of the DNA:DNA duplex, which resulted in increased BSI signal (Figure 9).

In addition to structural changes, the exchange of the water molecules that hydrate the soluble molecules upon binding is thought to influence the RI, which would have direct implications for BSI signal generation. It has been predicted based on NMR structure measurements of LNA:RNA hybrids that the number of water molecules interacting with the minor groove may be increased compared to DNA:RNA hybrids (27). The structure of an A-form hybrid may produce a larger BSI signal than B-form due to this exchange of waters of hydration from the solvent to the molecules, accounting in part for the improved BSI sensitivity when using the LNA probe. Continued efforts are aimed at identifying the role of waters of hydration on the shift of RI that occurs when an oligonucleotide probe hybridizes to an RNA target.

The results of these studies outline a set of optimal characteristics of nucleic acid probes for BSI detection of a viral RNA biomarker. It was determined that multiple nucleic acid probes, 22 nt in length, designed to target regions distributed across the RNA target resulted in the greatest BSI signal. These studies also indicate that the folding of the RNA target as well as the formation of the secondary structure geometry contributes substantially to BSI sensitivity for RNA detection. There is evidence that *mfold* software can be used to identify regions of unpaired nucleotides in RNA targets that are likely to produce high signal upon binding. Additional studies aimed at determining tertiary structure contributors to signal enhancement along with the secondary structure predictions of *mfold* could be useful for the rational

design of oligonucleotide probes for BSI detection. Additionally, it was determined that the induction of altered helical geometry of nucleic acids upon probe binding significantly improves BSI signal. We found that this can be achieved using LNA probes or a high background concentration of TFE, which promote formation of A-form structure in nucleic acids. Future work will focus on strategies to further enhance BSI sensitivity and specificity for RNA biomarkers, which could pave the way for a clinically relevant BSI assay for the detection of viral RNA in patient samples.

SUPPLEMENTARY DATA

Supplementary Data are available at NAR Online: Supplementary Table 1 and Supplementary Figures 1 and 2.

FUNDING

Bill & Melinda Gates Foundation through the Global Health Grand Challenges in Global Health initiative to F.R.H. and D.W.W.; a Vanderbilt University Discovery Grant to F.R.H and D.J.B.; the National Science Foundation [CHE 0848788 to D.J.B.]; and the National Science Foundation Graduate Research Fellowship Program [DGE 0909667 to N.M.A.]. Funding for open access charge: Bill & Melinda Gates Foundation through the Global Health Grand Challenges in Global Health initiative.

Conflict of interest statement. D.J.B. has a financial interest in a company that is commercializing BSI.

REFERENCES

1. Bordelon,H., Adams,N.M., Klemm,A.S., Russ,P.K., Williams,J.V., Talbot,H.K., Wright,D.W. and Haselton,F.R. (2011) Development of a low-resource RNA extraction cassette based on surface tension valves. *ACS Appl. Mater. Interfaces*, **3**, 2161–2168.
2. Bae,H.-G., Nitsche,A., Teichmann,A., Biel,S.S. and Niedrig,M. (2003) Detection of yellow fever virus: a comparison of quantitative real-time PCR and plaque assay. *J. Virol. Methods*, **110**, 185–191.
3. Jayagopal,A., Halfpenny,K.C., Perez,J.W. and Wright,D.W. (2010) Hairpin DNA-functionalized gold colloids for the imaging of mRNA in live cells. *J. Am. Chem. Soc.*, **132**, 9789–9796.
4. Mehlmann,M., Dawson,E.D., Townsend,M.B., Smagala,J.A., Moore,C.L., Smith,C.B., Cox,N.J., Kuchta,R.D. and Rowlen,K.L. (2006) Robust sequence selection method used to develop the FluChip diagnostic microarray for influenza virus. *J. Clin. Microbiol.*, **44**, 2857–2862.
5. Marras,S.A.E., Tyagi,S. and Kramer,F.R. (2006) Real-time assays with molecular beacons and other fluorescent nucleic acid hybridization probes. *Clin. Chim. Acta*, **363**, 48–60.
6. Nam,J.-M., Stoeva,S.I. and Mirkin,C.A. (2004) Bio-Bar-Code-based DNA detection with PCR-like sensitivity. *J. Am. Chem. Soc.*, **126**, 5932–5933.
7. Zhang,J., Lang,H.P., Huber,F., Bietsch,A., Grange,W., Certa,U., McKendry,R., Guntherodt,H.J., Hegner,M. and Gerber,C. (2006) Rapid and label-free nanomechanical detection of biomarker transcripts in human RNA. *Nat. Nanotechnol.*, **1**, 214–220.
8. Springer,T., Piliarik,M. and Homola,J. (2010) Surface plasmon resonance sensor with dispersionless microfluidics for direct detection of nucleic acids at the low femtomole level. *Sensor. Actuator. B Chem.*, **145**, 588–591.
9. Bornhop,D.J., Latham,J.C., Kussrow,A., Markov,D.A., Jones,R.D. and Sorensen,H.S. (2007) Free-solution, label-free molecular interactions studied by back-scattering interferometry. *Science*, **317**, 1732–1736.
10. Kussrow,A., Enders,C.S., Castro,A.R., Cox,D.L., Ballard,R.C. and Bornhop,D.J. (2010) The potential of backscattering interferometry as an in vitro clinical diagnostic tool for the serological diagnosis of infectious disease. *Analyst*, **135**, 1535–1537.
11. Kussrow,A., Enders,C.S. and Bornhop,D.J. (2011) Interferometric methods for label-free molecular interaction studies. *Anal. Chem.*, **84**, 779–792.
12. Olmsted,I.R., Xiao,Y., Cho,M., Csordas,A.T., Sheehan,J.H., Meiler,J., Soh,H.T. and Bornhop,D.J. (2011) Measurement of aptamer-protein interactions with back-scattering interferometry. *Anal. Chem.*, **83**, 8867–8870.
13. Latham,J.C., Markov,D.A., Sorensen,H.S. and Bornhop,D.J. (2005) Photobiotin surface chemistry improves label-free interferometric sensing of biochemical interactions. *Angew. Chem.*, **118**, 969–972.
14. Baksh,M.M., Kussrow,A.K., Mileni,M., Finn,M. and Bornhop,D.J. (2011) Label-free quantification of membrane-ligand interactions using backscattering interferometry. *Nat. Biotechnol.*, **29**, 357–360.
15. Pesciotta,E.N., Bornhop,D.J. and Flowers,R.A. II (2011) Back-scattering interferometry: a versatile platform for the study of free-solution versus surface-immobilized hybridization. *Chem.–Asian J.*, **6**, 70–73.
16. Perez,J.W., Vargis,E.A., Russ,P.K., Haselton,F.R. and Wright,D.W. (2011) Detection of respiratory syncytial virus using nanoparticle amplified immuno-polymerase chain reaction. *Anal. Biochem.*, **410**, 141–148.
17. Perez,J.W., Haselton,F.R. and Wright,D.W. (2009) Viral detection using DNA functionalized gold filaments. *Analyst*, **134**, 1548–1553.
18. Markov,D., Begari,D. and Bornhop,D.J. (2002) Breaking the 10-7 barrier for RI measurements in nanoliter volumes. *Anal. Chem.*, **74**, 5438–5441.
19. Vester,B. and Wengel,J. (2004) LNA (Locked Nucleic Acid): high-affinity targeting of complementary RNA and DNA. *Biochemistry*, **43**, 13233–13241.
20. Petersen,M., Bondensgaard,K., Wengel,J. and Jacobsen,J.P. (2002) Locked Nucleic Acid (LNA) Recognition of RNA: NMR solution structures of LNA:RNA hybrids. *J. Am. Chem. Soc.*, **124**, 5974–5982.
21. Ivanov,V.I., Minchenkova,L.E., Minyat,E.E., Frank-Kamenetskii,M.D. and Schyolkina,A.K. (1974) The B to A transition of DNA in solution. *J. Mol. Biol.*, **87**, 817–833.
22. Kypr,J., Kejnovska,I., Renciuk,D. and Vorlickova,M. (2009) Circular dichroism and conformational polymorphism of DNA. *Nucleic Acids Res.*, **37**, 1713–1725.
23. Wiese,K.C. and Hendriks,A. (2006) Comparison of P-RnaPredict and mfold–algorithms for RNA secondary structure prediction. *Bioinformatics*, **22**, 934–942.
24. Braasch,D.A. and Corey,D.R. (2001) Locked nucleic acid (LNA): fine-tuning the recognition of DNA and RNA. *Chem. Biol.*, **8**, 1–7.
25. Robertson,K.L. and Thach,D.C. (2009) LNA flow-FISH: a flow cytometry-fluorescence in situ hybridization method to detect messenger RNA using locked nucleic acid probes. *Anal. Biochem.*, **390**, 109–114.
26. Tran Tan,T., Pawestri,H., My,N., Minh,H., Syahrial,H., Vu,T., van Doorn,H.R., Wertheim,H., Van Vinh,C., Quang,H. *et al.* (2010) A real-time RT-PCR for detection of clade 1 and 2 H5N1 influenza A virus using Locked Nucleic Acid (LNA) TaqMan probes. *Virol. J.*, **7**, 46.
27. Nielsen,K.E., Rasmussen,J., Kumar,R., Wengel,J., Jacobsen,J.P. and Petersen,M. (2004) NMR studies of fully modified Locked Nucleic Acid (LNA) hybrids: solution structure of an LNA:RNA hybrid and characterization of an LNA:DNA hybrid. *Bioconjugate Chem.*, **15**, 449–457.